



SACRED HEART RESEARCH PUBLICATIONS

# Journal of Functional Materials and Biomolecules

Journal homepage: [www.shcpub.edu.in](http://www.shcpub.edu.in)



ISSN: 2456-9429

## Modification of properties of potassium bromide crystals in the growth medium of aqueous solution of L-arginine

J.Uma Maheswari<sup>\*1</sup>, C.Krishnan<sup>2</sup>, S.Kalyanaraman<sup>3</sup> and P.Selvarajan<sup>4</sup>

Received on 21 Jan 2017, Accepted on 27 Feb 2017

### ABSTRACT

Optical quality single crystals of potassium bromide were grown in the aqueous solution of L-arginine by slow solvent evaporation technique at room temperature (30 °C). The Face Centered Cubic structure of the grown crystal was elucidated by single crystal X-ray diffraction (SCXRD) study. The percentages of composite elements of grown material were studied through Energy Dispersive X-ray (EDX) spectrum. The Scanning Electron Microscope (SEM) reveals microstructural property of title compound crystal. The Fourier Transform infrared spectrum (FTIR) ensures the intermolecular interaction in the sample material. The optical transmission spectrum confirms wide range of transmission in UV-Vis-NIR region. The Z-scan technique reveals the third order nonlinear susceptibility  $\chi^{(3)}$ , refractive index ( $n_2$ ) and absorption coefficient ( $\beta$ ) of the sample. The thermogravimetric (TG) and differential thermogravimetric (DTA) analyses confirm the thermal stability of title compound up to 230 °C. The Vickers microhardness test reveals the appreciable mechanical strength of the crystal. The dielectric study ensures enhanced electrical properties of the grown crystal.

**Key words:** Bulk single crystal; X-ray diffraction; Optical susceptibility; Mechanical strength; Dielectric property.

### 1 Introduction

Crystalline compounds of organic, inorganic and semiorganic materials with the third harmonic generation efficiency spurt in the field of photonics and optoelectronics for the past two decades. The potential applications of third harmonic NLO materials in laser radiation production, optical switching, optical information storage, optical limiters, optical logic gates etc [1, 2] were remarkable. Crystals of organic materials with high second harmonic generation (SHG) efficiency and absorption wavelength up to visible region exhibit a yellow or orange colour. Hence found no use in wavelength conversion of semiconductor lasers. The hybrid material of organic and inorganic compound-semiorganic materials emerged with advantages of high resistance to laser damage threshold, large

hyperpolarizability, and fast response to electro-optic devices, narrow transparency widow and good thermal and mechanical properties [3]. An excessive investigation have been made on L-arginine compounds, all formed acentric crystals and hence produced large nonlinearity with less angular sensitivity in the phase matching conditions [4]. L-Arginine, a strong amino acid produced some notable NLO materials such as L-arginine trifluoroacetate [5], L-arginine acetamide [6], KDP crystal doped with L-arginine [7] & L-arginine maleate dihydrate [8].

In the present investigation, an attempt has been made to grow potassium bromide crystals in the growth medium of aqueous solution of L-arginine (PBLA) and grown successfully with third harmonic efficiency and are expected to find use in photonic device fabrication. The interactions between L-arginine cations through hydrogen bonds are possible since it contains positively charged protonated guanidyl group and  $\alpha$  - amino group and negatively charged carboxylate group. The unique changes observed in the physical properties of potassium bromide may due to L - arginine. The title compound was characterized through X- ray diffraction, optical, Z-scan, FT-IR, mechanical, thermal studies and dielectric analyses.

### 2 Experimental

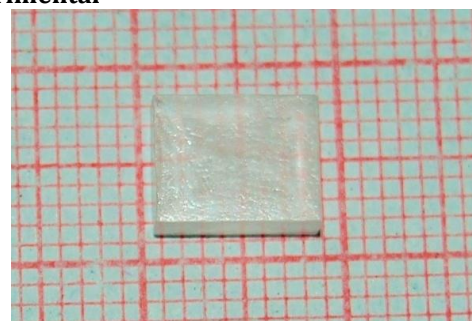


**Fig.1:** The photograph of grown PBLA crystal

\* Corresponding author: E-mail address: [umak.anand@gmail.com](mailto:umak.anand@gmail.com) (J.Uma Maheswari), Phone: +91-7598551455

<sup>1</sup> Department of Physics, The M.D.T.Hindu College, Tirunelveli – 627010, Tamilnadu, India.

<sup>2</sup> Department of Physics, Arignar Anna College, Aralvoymoli – 629301, Tamilnadu, India.

<sup>3</sup> Physics Research Centre, Sri Paramakalyani College, Alwarkurichi– 627412, Tamilnadu, India.

<sup>4</sup> Department of Physics, Aditanar College of Arts and Science, Tiruchendur- 628216, Tamilnadu, India.

The title compound was synthesized by dissolving high purity potassium bromide and L - arginine in distilled water in the ratio of 2:1. The resulting solution was stirred well of about two hours and filtered to allow crystallization by slow solvent evaporation method at room temperature. Bulk single crystals of size of about 8 x 7 x 4 mm<sup>3</sup> (Fig.1) were harvested after a span of 30 days with good quality.

The cell parameters and space group of grown PBLA crystal were obtained from single crystal X-ray diffraction (SCXRD) studies carried out by Enraf Nonius CAD4- MV31 single crystal X-ray diffractometer with CuK $\alpha$  ( $\lambda=1.5406 \text{ \AA}$ ) radiation. The powder X-ray diffraction of the powdered sample was taken by PANalytical X'pert Pro powder X'celerator diffractometer. The microstructure of PBLA crystal was studied using Jeol JSM6390 scanning microscope and EDS - INCA, Oxford instruments, UK employed to ensure the composite elements of title compound. The Perkin Elmer spectrometer in the range 400 - 4000 cm<sup>-1</sup> was used to record FTIR spectrum at a resolution of 4 cm<sup>-1</sup> and UV-Vis -NIR spectrometer (Varian, Carry 5000) was used to carry out optical transmission spectrum in the range 190 - 1100 nm. The Z - scan technique was employed with a He - Ne laser ( $\lambda = 632.8 \text{ nm}$ ) source and with a lens of 22.5 cm focal length. The Perkin Elmer Thermal analyzer at a heating rate of 40 - 730° C at 20° C/min used to analyze thermogravimetric (TG) and differential thermogravimetric (DTA) of the sample material. The impedance spectroscopy was executed on PBLA material by using an impedance analyzer (Model: ZAHNER-IM6/Germany- electrochemical work station).

### 3 Results and Discussion

#### 3.1 X-ray diffraction and EDX analyses

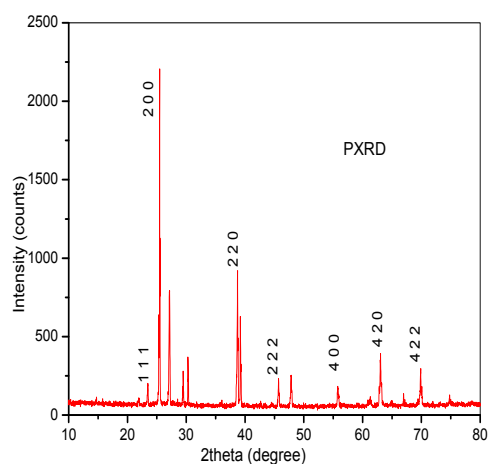


Fig.2: The PXRD pattern of PBLA crystal

The single crystal X-ray diffraction data of PBLA crystal indicates that it crystallizes in cubic system with Fm3m space group. The obtained lattice parameter values and volume of the grown title compound were  $a = b = c = 6.63$

$\text{\AA}$ ,  $\alpha = \beta = \gamma = 90^\circ$ ,  $V = 292 \text{ \AA}^3$ . The powder X-ray diffraction pattern of the powder sample shown in Fig.2 was carried out with CuK $\alpha$  radiation of  $\lambda=1.5406 \text{ \AA}$  in the range  $2\theta$  at a scan rate of  $3^\circ / \text{sec}$ . The XRD pattern - a finger print of a crystalline substance confirms that PBLA crystal belongs to cubic crystal system. The introduction of new hkl plane d-spacing due to nonuniform distortion may cause the few additional peaks in the pattern. However the sharp and high intensity peaks of PXRD pattern confirms that the grown PBLA crystal has high crystalline nature. Thus the (200), (020) and (002) planes of cubic cell were in same spacing and form only one line called the (200) line. The cell parameters, crystal structure and volume obtained from UNITCELL software ensure SCXRD results.

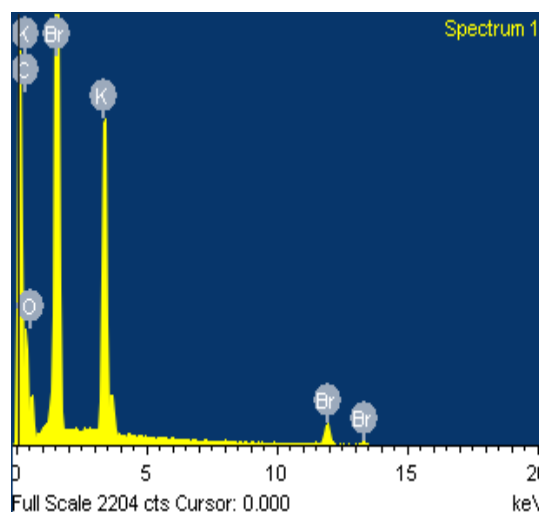


Fig.3: EDX spectrum of PBLA crystal

The recorded EDX spectrum was shown in Fig.3 which confirms the new composite elements in the PBLA crystal. The higher atomic number elements were tabulated in Table 1. The SEM micrograph as shown in Fig.4 investigates the surface morphology of the grown material.

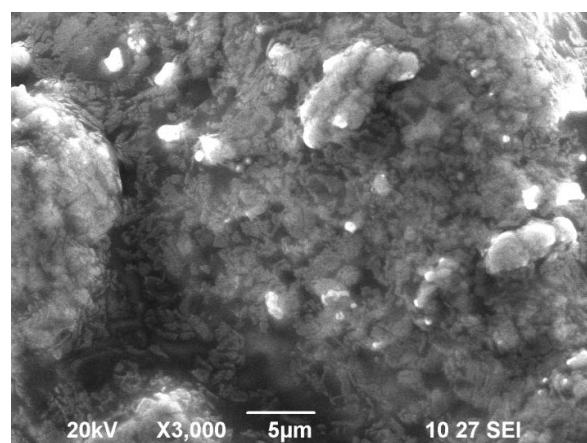
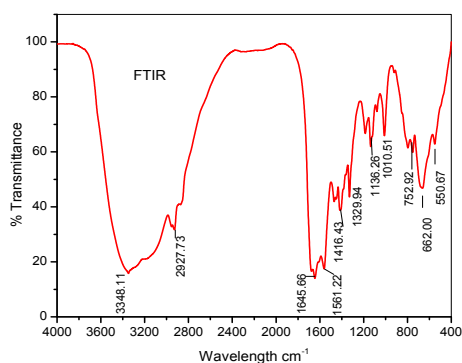


Fig.4: Scanning electron micrograph of PBLA crystal

**Table 1:** Elements in the grown PBLA crystal

Elements	Weight %	Atomic %
Carbon	53.9	78.73
Oxygen	9.58	10.58
Potassium	10.92	4.94
Bromine	26.00	5.75

### 3.2 Fourier Transform Infrared analysis

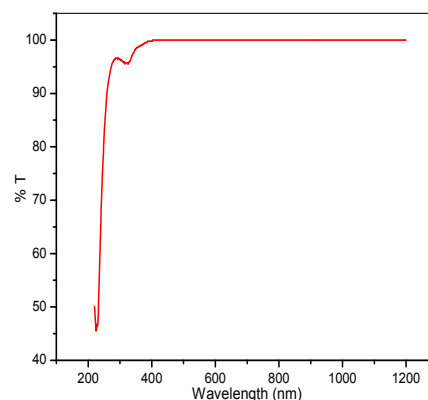
**Fig.5:** The IR spectrum of grown PBLA crystal**Table 2:** Vibrational spectral data and assignments of PBLA crystalWave number (cm<sup>-1</sup>) - Assignment

3348.11	- N-H vibration from NH <sub>2</sub> and NH <sub>3</sub> <sup>+</sup>
2954.69	-CH <sub>2</sub> symmetric stretching
2927.73	-Associated with CH <sub>2</sub> lines of L-arginine
1676.77	- Out of plane bending of NH <sub>2</sub> group / C = N stretch
1645.66	- COO <sup>-</sup> asymmetric bend / NH <sub>2</sub> asymmetric bend
1561.22	-NH <sub>3</sub> <sup>+</sup> symmetric bend / C - H and C - N stretch
1469.36	- C - H and N - H rocking
1416.43	- CH <sub>2</sub> asymmetric stretch / COO <sup>-</sup> symmetric bend
1329.94	-OH bending vibration bands / COO <sup>-</sup> asymmetric stretch
1185.57	-NH <sub>3</sub> <sup>+</sup> rocking
1136.26	-NH <sub>2</sub> wagging
1079.01	-C - N stretch
1010.51	-Stretching of CH of CH <sub>3</sub> group
796.41	- Br-O stretch / stretch of CNH group / CH <sub>2</sub> rock
752.92	-NH wagging
662.00	-C-Br symmetric stretch / COO <sup>-</sup> in plane bend
550.67	- K-O stretching / COO <sup>-</sup> rocking / NH <sub>3</sub> <sup>+</sup> in plane rocking

The infrared spectrum for grown PBLA crystal is depicted in Fig.5. The spectrum prudent the absence of water molecules as there is no peak owing to OH stretch at 3400 cm<sup>-1</sup> [9]. The charged L-arginine can be distinguished

by the protonated guanidyl group [(H<sub>2</sub>N)<sub>2</sub> CNH]<sup>+</sup> i.e., the amino group (NH<sub>3</sub><sup>+</sup>) and the deprotonated carboxylate group (COO<sup>-</sup>) [10 - 12]. The N-H stretching vibration at 3348.11 cm<sup>-1</sup> is due to NH vibration from N-H and NH<sub>3</sub><sup>+</sup> of guanidyl group [13]. The weak absorption lines at 2927.73 cm<sup>-1</sup> and at 1676.77 cm<sup>-1</sup> were owing to CH<sub>2</sub> and out of plane bending of NH<sub>2</sub> group of L-arginine respectively. Owing to stretching vibration of Br-O bonds an absorption peak raised at 796.41 cm<sup>-1</sup> and the peak at 550.67 cm<sup>-1</sup> was owing to K-O rocking and the strong band at 662 cm<sup>-1</sup> may due to C-O stretch [14, 15]. Table 2 represents the observed peak assignment of grown PBLA crystal.

### 3.3 Optical transmission analysis

**Fig.6:** Optical transmission spectrum of PBLA crystal

Transmission range of PBLA crystal is essential for the use in optoelectronics. The spectrum of optical transmission was depicted in the Fig.6. The grown crystal has UV cut-off around 224 nm may due to electronic excitation in COO<sup>-</sup> group. An absorption peak around 320 nm may assigned due to  $\pi - \pi^*$  transitions in azo methyne group. The band gap energy is calculated using the formula  $E_g = hc / \lambda$  and found to be 5.55 eV, which is the characteristic value of dielectric materials [16] and indicates the presence of L - arginine decreases transmission percentage in KBr, hence results moderate  $E_g$  value as desired for dielectric materials [17]. On the other hand, the sample material has a wide transparency window between 400-1100 nm confirms grown sample suitability in parametric oscillation, in particular NLO applications. The grown sample PBLA has better transmission than reported L - arginine and L - arginine added compounds such as, L - arginine monohydrochloride monohydrate (LAHCL) [18], zinc tris (thiourea) sulphate [19] and potassium dihydrogen phosphate [20].

### 3.4 Nonlinear optical analysis

The third order nonlinear optical measurements were investigated by Z-scan technique. The normalized transmittance and sample position in mm of title compound for both open and closed aperture were

depicted in Fig.7 and Fig.8 respectively. In terms of the on-axis phase shift  $|\Delta\Phi|$ , the transmittance difference between the pre-focal transmittance maximum (peak) and post-focal minimum (valley)  $\Delta T_{p-v}$  can be written as

$$\Delta T_{p-v} = 0.406 (1-S)^{0.25} |\Delta\Phi| \quad (1)$$

Where S, the linear transmittance of the aperture is expressed as

$$S = 1 - \exp(-2r_a^2 / \omega_a^2) \quad (2)$$

Where  $r_a$  denotes aperture radius and  $\omega_a$  denotes beam radius at the aperture.

The third order nonlinear optical refractive index  $n_2$  of the crystal can be calculated using the relation [21]

$$n_2 = |\Delta\Phi| / kI_0L_{\text{eff}} \quad (3)$$

With  $k = 2\pi / \lambda$ ,  $\lambda$  is the laser beam wavelength and  $I_0$  is the laser beam intensity.

Where  $L_{\text{eff}}$  implies the effective thickness of the crystal as

$$L_{\text{eff}} = [1 - \exp(-\alpha L)] / \alpha \quad (4)$$

Where  $\alpha$  and L can be denoted as linear absorption coefficient and thickness of the sample respectively. The material nonlinear absorption coefficient  $\beta$  expressed as

$$\beta = 2\sqrt{2}\Delta T / I_0L_{\text{eff}} \quad (5)$$

Where  $\Delta T$  is consider to be one valley value at the open aperture curve of Z-scan. The real and imaginary part of third order non linear optical susceptibility  $\chi^{(3)}$  can be expressed as

$$\text{Re } \chi^{(3)} (\text{esu}) = 10^{-4} (\epsilon_0 C^2 n_0^2 n_2) / \pi \quad (6)$$

$$\text{Im } \chi^{(3)} (\text{esu}) = 10^{-2} (\epsilon_0 C^2 n_0^2 \lambda \beta) / 4\pi^2 \quad (7)$$

$$|\chi^{(3)}| = [(\text{Re } \chi^{(3)})^2 + (\text{Im } \chi^{(3)})^2]^{1/2} \quad (8)$$

Where  $\epsilon_0$  and C were permittivity and light velocity of vacuum and  $n_0$  is the linear refractive index of the sample.

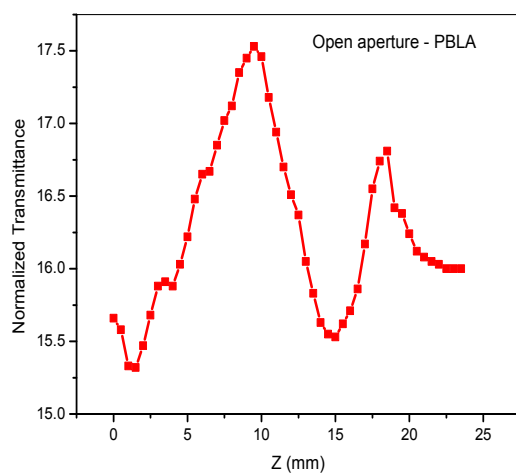


Fig.7: Open aperture z-scan curve of PBLA crystal

The calculated  $n_2$  is  $-2.5 \times 10^{-10} \text{ cm}^2/\text{W}$ , which infers the self-defocusing nature since the closed aperture curve shows pre-focal peak followed by post-focal valley and the  $\beta$  value is  $2.25 \times 10^{-5} \text{ cm/W}$ , which may be evident for many delocalized  $\pi$  electrons produced from protonated amino group in crystal lattice [22]; hence the polarization and nonlinear optical susceptibility were enhanced. The  $\pi$ -electron cloud movement from the donor to acceptor in the compound material gives rise to  $\chi^{(3)} = 2.31 \times 10^{-8} \text{ esu}$  and may find application in photonic and optical devices. The title compound has better third order nonlinear susceptibility than  $\text{KBe}_2\text{BO}_3\text{F}_2$  ( $\chi^{(3)} = 0.99 \times 10^{-13} \text{ esu}$ ) and  $\text{LiKB}_4\text{O}_7$  ( $\chi^{(3)} = 4.858 \times 10^{-9} \text{ esu}$ ) crystals [23, 24]. Table 3 represents the parameter values from Z-scan measurements on PBLA crystal.

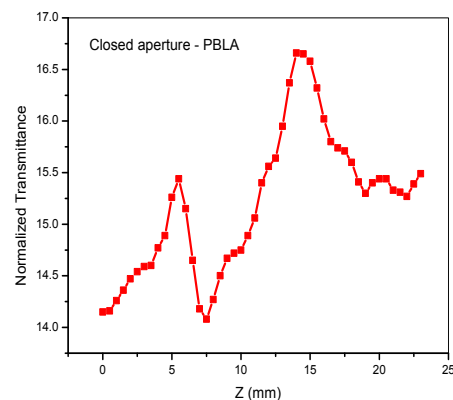
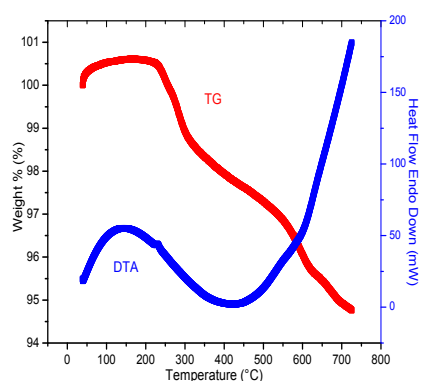


Fig.8: Closed aperture Z-scan curve of PBLA crystal

Table 3: The obtained parameter values from Z-scan technique on PBLA crystal

Parameter	Measured values of PBLA crystal
Laser beam wavelength, $\lambda$	632.8nm
Focal length of lens, f	22.5 cm
Aperture radius, $r_a$	4 mm
Spot size diameter in front of the aperture, $\omega_a$	1 cm
Incident intensity at the focus, Z = 0	2 MW/cm <sup>2</sup>
Effective thickness, $L_{\text{eff}}$	1.1 mm
Non linear absorption coefficient, $\beta$	$2.25 \times 10^{-5} \text{ cm/W}$
Nonlinear refractive index, $n_2$	$-2.5 \times 10^{-10} \text{ cm}^2/\text{W}$
Third order nonlinear optical susceptibility, $\chi^{(3)}$	
Real part of $\chi^{(3)}$	$2.31 \times 10^{-8} \text{ esu}$
Imaginary part of $\chi^{(3)}$	$2.1 \times 10^{-8} \text{ esu}$
	$9.53 \times 10^{-9} \text{ esu}$

### 3.5 Thermal analysis



**Fig.9:** TG/DTA curves of PBLA crystal

The thermogravimetric and differential gravimetric analysis were carried out from 40 °C to 730 °C in the presence of nitrogen gas. The Fig.9 represents TG/DTA curves, where the TG curve shows no weight loss in the sample up to 230 °C; hence the sample has absence of physically observed water or of lattice water is an impressive feature. The DTA curve shows no exothermic or endothermic peak below 226.44 °C, indicates the sample crystal may have no isomorphous transitions below the decomposition temperature [25] and conventionally more lattice force in the crystal lattice. The grown PBLA crystal has appreciable thermal stability than pure L - arginine diphosphate (191 °C) [26] and L - arginine diiodate (142 °C) [27] crystals as required for device fabrication. The observed weight loss in the temperature range 230 °C – 300 °C due to the decomposition of the compound material [28]. The continuation of decomposition curve up to 730 °C shows the removal of gaseous products [29]. Also PBLA crystal is suitable for laser application where the materials required are to withstand high temperature, in account of no decomposition observed up to the melting point.

### 3.6 Vickers microhardness test

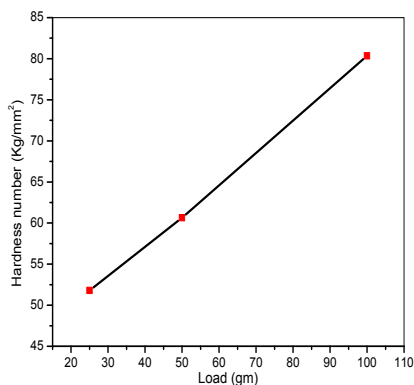


**Fig.10:** Plot of load versus Vickers hardness number of PBLA crystal

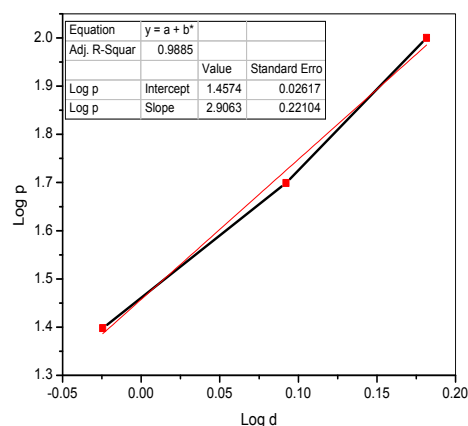


**Fig.11:** Plot of Log d versus Log p of PBLA crystal

The physical properties of crystalline materials like mechanical strength which estimates the material performance as a device. Reverse indentation size effect [30] observed from Fig.10 which illustrates microhardness  $H_v$  against applied load  $P$ , evident appreciable crystalline perfection; hence the sample requires greater stress to generate dislocation. Cracks may form on the surface of grown crystal beyond 100 g load due to release of internal stresses produced by indentation [31]. The work hardening coefficient of the title compound material was estimated using the Meyer's relation  $P = ad^n$  [32], where  $P$  is the applied load, 'a' is a constant, 'd' is the diagonal length of indentation and 'n' is the work hardening coefficient. The plot log  $P$  against log  $d$  is a straight line, which is shown in Fig.11. The value of  $n$  is found to be 2.906 and hence the grown PBLA crystal belongs to soft category [33]. The grown PBLA crystal is harder than the L - Arg: HCl (62.69 kg/mm<sup>2</sup>), L - Arg: HBr (47.98 kg/mm<sup>2</sup>) and potassium thiourea chloride (74 kg/mm<sup>2</sup>) and can find application in device fabrication.

### 3.7 Dielectric properties

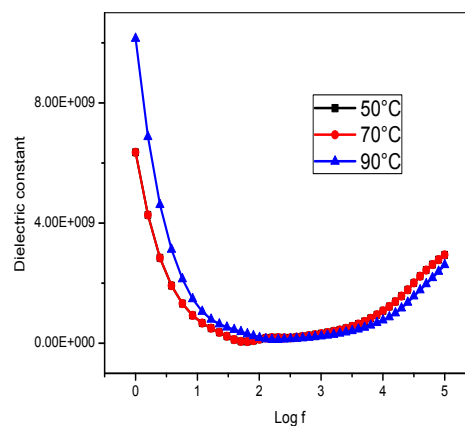


**Fig.12:** Dielectric constant variations with log frequency of PBLA crystal

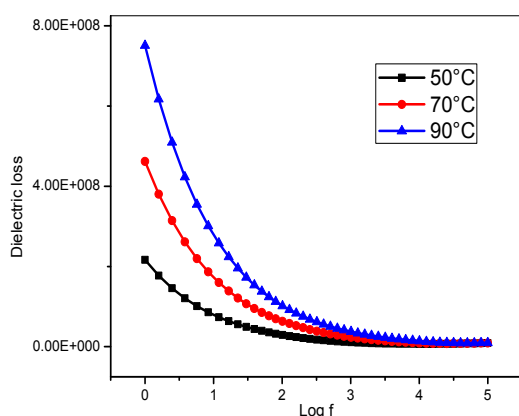


**Fig.13:** Dielectric loss variations with log frequency of PBLA crystal

The presence of space charge, orientational ionic and electronic polarizations may cause high dielectric constant values at low frequencies and gradual decrease of these polarizations may cause low value of dielectric constant at higher frequencies. At low frequency region, space charge polarization is predominant among the four polarizations [34, 35]. The increase of dielectric constant with temperature is a facet of crystal expansion, crystal defects and ionic and electronic polarizations [36, 37]. The small variation of dielectric constant with temperature was observed in Fig.12, which deduces that the grown PBLA crystal is of favorable chemical homogeneity [38]. The plot of dielectric loss with frequency for various temperatures shown in Fig.13, which infers that the grown sample has higher optical quality with lesser defects since the dielectric loss is low at high frequencies and high at low frequencies [39]. Hence, the grown sample may use in NLO based device applications [40] and the higher dielectric constant values than SF crystals [41] suggest adopt in capacitor technology. The sample material has better dielectric behaviour than LAA and LAO crystals [42].

#### 4 Conclusions

Good optical quality single crystals of potassium bromide in the growth medium of aqueous solution of L-arginine were grown successfully by slow solvent evaporation technique at room temperature. The SCXRD study ensures centrosymmetric cubic structure of grown PBLA crystal with Fm3m space group and the PXRD study confirms the crystallinity. The composite elements of grown material were identified by EDX spectrum. The FTIR spectrum ensures the intermolecular interactions and functional groups presence in PBLA crystal. The UV-Vis-NIR spectrum shows a sharp lower absorption peak at around 224 nm may due to electronic excitation in COO-group of L - arginine. A characteristic  $E_g$  value of dielectric material is obtained as 5.55 eV. The essential Z-scan measurement of PBLA crystal gives the third order nonlinear optical susceptibility  $\chi^{(3)}$ , refractive index  $n_2$  and absorption coefficient  $\beta$  are of the order of  $2.31 \times 10^{-8}$  esu,

$-2.5 \times 10^{-10}$  cm<sup>2</sup>/W, and  $2.25 \times 10^{-5}$  cm/W, which reveals the grown sample nature of self defocusing and multi photon absorption process and are suitable for optical switching and limiting. The TG / DTA thermograms reveal that the sample material has good thermal stability. The Vickers microhardness test on title compound shows reverse indentation size effect and belongs to soft category materials in accordance to Meyer. The high dielectric constant value of PBLA crystal suggests use in capacitor technology. The dielectric loss and dielectric constant decrease with increase of frequency and low values at high frequencies exhibit the desired NLO property of the crystal for device application. All observed properties of PBLA crystal was compared with other reported compounds and results better.

#### Acknowledgements

The authors acknowledge NIT Trichy for Z-scan measurements and IIT Madras for single crystal X-ray diffraction studies. One of the authors (J.Uma Maheswari) acknowledges University Grants Commission (UGC) – Hyderabad, India for teacher fellowship under faculty development programme (XII-plan 2012-2017) and the management of The M.D.T.Hindu College, Tirunelveli, India.

#### References

- [1] Arunkumar and P. Ramasamy, J. Cryst. Growth 388 (2014) 124.
- [2] K. Ramya, N.T. Saraswathi and C. Ramachandra Raja, Optik 127 (2016) 2495.
- [3] R. Sankar, R. Muralidharan, C.M. Rahgavan, R. Mohankumar and R. Jayavel, Mater. Lett. 62 (2008) 133.
- [4] R. Muralidharan, R. Mohankumar, R. Jayavel and P. Ramasamy, J. Cryst. Growth 259 (2003) 321.
- [5] T. Pasanyaa, M. Haris, V. Mathivanan, M. Senthilkumar, T. Mahalingam and V. Jayarama krishnan, Mater. Chem. Phys. 147 (2014) 433.
- [6] B. Anitha, S. Rathakrishnan, P. Malliga and A. Joseph Arul Pragasam, J. Therm. Anal. Calorim. 119 (2015) 785.
- [7] I.M. Pritula, E.I. Kostenyukova, O.N. Bezkravnaya, M.I. Kolybaeva, D.S. Sofronov, E.F. Dolzhenkova, A. Kanaev and V. Tsurikov, Opt. Mater. 57 (2016) 217.
- [8] T. Baraniraj and P. Philominathan, Spectrochim. Acta A 75 (2010) 74
- [9] K. Meera, R. Muralidharan, R. Dhansakaran, Prapun Manyum and P. Ramasamy, J. Cryst. Growth 263 (2004) 510.
- [10] T. Mallik and T. Kar, J.Cryst. Growth 285 (2005) 178.
- [11] Z.H. Sun, D. Xu, X.Q. Wang, X.J. Liu, G. Yu, G.H. Zhang, L.Y. Zhu and H.L. Fan, Cryst. Res. Technol. 42 (2007) 812.
- [12] A.M. Petrosyan, Vib. Sepctrosc. 41 (2006) 97.
- [13] J.R. Govani, W.G. Durrer, Marian Manciuc, Cristian Botez, and Felicia S. Manciuc, J. Mater. Res. 24 (2009) 2316.

- [14] A.M. Petrosyan, H.A. Korapetyan, R.P. Sukiasyan, A.E. Aghajanyan, V.G. Morgunov, E.A. Kravchenko and A.A. Bush, *J. Mole. Struct.* 752 (2005) 144.
- [15] J. Uma Maheswari, C. Krishnan, S. Kalyanaraman and P. Selvarajan, *Physica B* 502 (2016) 32.
- [16] Sd. Zulifiqar Ali Ahamed, G.R. Dillip, P. Raghavaiah, K. Mallikarjuna and B. Deva Prasad Raju, *Arab. J. Chem.* 6 (2013) 429.
- [17] M.M. Khandpekar and S.P. Pati, *Opt. Commun.* 283 (2010) 2700.
- [18] K. Sangeetha, R. Ramesh Babu, G. Bhagavannarayana and K. Ramamurthi, *Spectrochim. Acta A* 79 (2011) 1017.
- [19] Sweta Moitra and Tanusree Kar, *Opt. Mater.* 30 (2007) 508.
- [20] P.V. Dhanaraj, S.K. Mathew and N.P. Rajesh, *J. Cryst. Growth* 310 (2008) 2532.
- [21] A. Shanthi, C. Krishnan and P. Selvarajan, *Spectrochim. Acta A* 122 (2014) 521.
- [22] R. Surekha, P. Sagayaraj and K. Ambujam, *Opt. Mat.* 36 (2014) 945.
- [23] Baichang Wu, Dingyuen Tang and Ning Ye, Chuangtian Chen, *Opt. Mater.* 5 (1996) 105.
- [24] M. Sukumar, R. Ramesh Babu and K. Ramamurthi, *Appl. Phys. B* 121 (2015) 369.
- [25] A. Joseph Arul Pragasam, J.Madhavan, M.Gulam Mohamed, S.Selvakumar, K. Ambujam and P. Sahayaraj, *Opt. Mater.* 29 (2006) 173.
- [26] Reena Ittyachan and P. Sagayaraj, *J. Cryst. Growth* 243 (2002) 356.
- [27] R. Sankar, R. Muralidharan, C.M. Raghavan and R. Jayavel, *Mater. Chem. Phys.* 107 (2008) 51.
- [28] N. Pattanaboonmee, P. Ramasamy, R. Yimnirun and P. Manyum, *J. Cryst. Growth* 314 (2011) 196.
- [29] S. Mukerji and T. Kar, *Mater. Res. Bull.* 33 (1998) 619.
- [30] K. Sangwal, *Mater. Chem. Phys.* 63 (2000) 145.
- [31] T. Uma Devi, N. Lawrence, R. Ramesh Babu and K. Ramamurthi, *J. Cryst. Growth* 310 (2008) 116.
- [32] Emilio Jimeno and Jose Terraza, The Meyer law for hardness tests, *Nature* (1950).
- [33] J. Mary Linet and S. Jerome Das, *Physica B* 405 (2010) 3955.
- [34] P. Selvarajan, B.N. Das, H.B. Gon and K.V. Rao, *J. Mater. Sci.* 29 (1994) 4061.
- [35] N.V. Prasad, G. Prasad, T. Bhimasankaram, S.V. Suryanarayana and G.S. Kumar, *Bull. Mater. Sci.* 19 (1996) 639.
- [36] K.V. Rao and A. Smakula, *J. Appl. Phys.* 36 (1965) 2031.
- [37] A.S.J. Lucia Rose, P. Selvarajan and S. Perumal, *Spectrochim. Acta A* 81 (2011) 270.
- [38] V.A. Hiremath and A. Venkataraman, *Bull. Mater. Sci.* 26 (2003) 391.
- [39] G. Anandha Babu, S. Sreedhar, S. Venugopal Rao and P. Ramasamy, *J. Cryst. Growth* 312 (2010) 1957.
- [40] R. Arivuselvi and A. Ruban Kumar, *Mat. Lett.* 178 (2016) 264.
- [41] C. Amuthambigai, C.K. Mahadevan and X. Sahaya Shajan, *J. Curr. Appl. Phys.* 16 (2016) 1030.
- [42] M. Meena and C.K. Mahadevan, *Mater. Lett.* 62 (2008) 3742.